Available online at www.sciencedirect.com
SCIENCE DIRECT®

Journal of the European Ceramic Society 23 (2003) 2931–2937
www.elsevier.com/locate/jeurceramsoc

Carbonated hydroxyapatite as bone substitute

E. Landi[a,*], G. Celotti[a], G. Logroscino[b], A. Tampieri[a]

[a]*Institute of Science and Technology for Ceramics- ISTEC-CNR, via Granarolo, 64 48018 Faenza, Italy*
[b]*Clinica Ortopedica Università Cattolica Sacro Cuore, Largo F. Vito 1 - 00185 Rome, Italy*

Abstract

B-carbonateapatite (CHA) powder was synthesized starting from calcium nitrate tetrahydrate, diammonium hydrogen phosphate and sodium hydrogen carbonate. The powder was fully characterized in terms of phase purity, stoichiometry, morphology, specific surface area and particle size distribution. The thermal stability of the powder in air and CO_2 atmosphere also was evaluated by thermal analysis. Electroacoustic analysis of the water based suspension of the CHA powder was used to determine the stability of the slurry. Porous bodies of CHA were prepared by impregnation of cellulose sponges with a proper slurry of the powder and optimizing the subsequent sintering. The fired samples were characterized in terms of phase purity and carbonate content, microstructure and pore size distribution. The compressive strength also was evaluated, resulting in 6.0 ± 0.5 MPa. First results of in vivo tests on New Zealand White rabbits showed good biocompatibility and osteointegration of the CHA implant, with higher osteoconductive properties and earlier bioresorption, compared to HA samples, used as control.

Keywords: Biomaterial; Carbonated hydroxyapatite; Porous ceramic; Bone tissue mimicking

1. Introduction

A key target of biomaterials research is the preparation of a synthetic carbonate containing hydroxyapatite (CHA) bone-substitute ceramic, that mimics the chemical composition of the natural hard tissue. The carbonate content in the bone mineral is about 4–8 wt.%[1] and it depends on the age of the individual.[2,3] Considering the hydroxyapatite structure, the carbonate group can substitute both the hydroxyl and the phosphate ions, giving rise to the A-type and B-type carbonation, respectively. The B-type is the preferential carbonate substitution found in the bone of a variety of species, with the A/B type ratio in the range 0.7–0.9.[4] A higher value of the A/B ratio was observed in old tissue, compared to young tissue.

The presence of B-carbonate in the apatite lattice was shown to cause a decrease in crystallinity and an increase in solubility in both in vitro and in vivo tests.[5] Moreover the A-CHA surface showed a lower affinity for the human trabecular osteoblastic cell, compared to HA; this is demonstrated by the lower cell attachment and collagen production which was attributed to a decrease of the polar component of the surface of the A-carbonated biomaterial.[6,7]

The carbonate substituted hydroxyapatite powder must not lose the carbonate content during eventual heat treatments or, alternatively, the carbonate loss must be controlled in order to assure an adequate residue, i.e. a carbonate amount similar to that of the biological hydroxyapatite (4–8 wt.%). Additionally, the carbonate substituted hydroxyapatite must be thermally stable such that it will not decompose to undesirable secondary phases upon calcining and sintering.

A porous ceramic structure is otherwise ideal for bone replacement as filler of both load-bearing and non-load bearing osseous defects, owing to its potential to repair the site through a complete penetration of the osseous tissue. The impregnation of cellulose sponges with HA powder suspension has been demonstrated to be effective to obtain porous bodies with adequate pore dimensions and distribution, which mimic the morphology of the spongy bone and favours the osteoconduction process.[8,9]

Starting from this impregnation method, various process parameters must be changed and optimised in order to produce CHA porous bodies; the most important are: a) the slurry concentration and stabilisation; b) the sintering temperature and atmosphere.

* Corresponding author. Tel.: +39-546-699-711; fax: +39-546-46381.
E-mail address: elena@irtec1.irtec.bo.cnr.it (E. Landi).

0955-2219/03/$ - see front matter © 2003 Published by Elsevier Ltd.
doi:10.1016/S0955-2219(03)00304-2

Finally, a good impregnation and a correct firing guarantee the best performances of the bioceramic to mimic bone porosity and composition and to provide sufficient mechanical properties.

2. Experimental

The synthesis of the CHA powder was performed starting from analytical grade Ca $(NO_3)_2$ 4 H_2O, $(NH_4)_2HPO_4$ and $NaHCO_3$ (Merck, Darmstadt, Germany). The amounts of reagents were chosen in order to maintain the Ca/P molar ratio 1.667 of stoichiometric hydroxyapatite: competition for entering the apatite structure was set up between phosphate and carbonate groups. 540 ml of a solution containing 0.15 mol of calcium nitrate tetrahydrate was prepared, with the final pH held at ≈12–13 by NH_4OH additions. A second solution was prepared by dissolving 0.09 mol of ammonium hydrogen phosphate into 480 ml of H_2O and then adding 0.06 mol of sodium hydrogen carbonate. The pH of the solution was then adjusted with NH_4OH additions and the total volume was brought to 960 ml with deionized water. The phosphate/carbonate solution was added drop-wise over 2 h to the calcium solution, which was kept at 95 °C and under mechanical stirring. During the reaction process the pH was continuously controlled and stabilised at >11 with NH_4OH additions (about 280 ml in total). The suspension was then maintained at 90 °C and stirred for 24 h and finally aged for 24 h. The precipitate was washed (with about 600 ml of deionised water) and filtered under vacuum for three times, air dried at 80 °C and finally sieved at 400 and 150 μm.

The specific surface area of the powder was evaluated by the Brunauer-Emmett-Teller method (Sorpty 1750, Carlo Erba, Milan, Italy). For particle size distribution measurement, the powder was analysed by sedimentography (Sedigraph 5100, Micromeritics, Norcross, GA) after ultrasonic dispersion for 10 min. In order to evaluate Ca/P ratio, inductively coupled plasma-optical emission spectrometry (ICP-OES) analysis was performed (Liberty 200, Varian, Clayton South, Australia). Fourier transformed infrared (FTIR) spectroscopy (FT-IR 1750, PerkinElmer Instruments, Shelton, CT, USA) also was performed to determine HA stoichiometry deviations, i.e., the presence of carbonate anions partially substituting for PO_4^{3-} and/or OH^- groups.

The elemental analyser (LECO C/S, Leco Corporation, St. Joseph, MI, USA) was used to evaluate the carbon content of the powder and consequently to estimate the carbonate amount.

Simultaneous thermal analysis (STA 409 Netzsch Geraetebau GmbH, Selb, Germany) was used in order to follow the thermal transformation process and the thermal stability of the powder in air and carbon dioxide atmospheres.

The morphological evaluation of the powder and microstructural characterisation of the sintered porous bodies was performed by scanning electron microscopy (SEM; Stereoscan 360, Leica, Cambridge, UK). Specimens also were characterized by X-ray diffraction (Cu Kα radiation, Miniflex Rigaku, Tokyo, Japan) to evaluate the degree of crystallinity of the powder, the crystalline phase composition and the carbonation degree of the powder and the sintered bodies.

Zeta-potential determination of the CHA powder was carried out with an electroacoustic technique, using an electrokinetic sonic amplitude (ESA) measurement apparatus (Acoustosizer, Colloidal Dynamics, Sydney, Australia). The suspension sample was prepared by ball milling the powder for 1 h into a 10^{-2} M KCl solution to maintain a constant ionic strength. A fixed concentration of 3 vol% solid was used and the suspension, placed in the measurement cell, was kept under constant stirring at 25 °C. The aqueous dispersing behavior of the CHA powder was investigated through potentiometric titration. An automatic titration software was used to measure the ζ potential and conductivity as a function of pH (HNO_3 1M and KOH 1M were used to adjust the pH). The isolectric point (IEP) was identified at the pH axis crossing point.

Porous samples were prepared by soaking natural cellulose sponges (Spontex, Verniano, Italy) in 21 vol.% CHA water based suspension, containing 1.2 wt.% Dolapix CA (Zschimmers & Schwartz) as a dispersing agent. After soaking, the sponges were left to dry in open air for 24 h and then sintered. With the aid of thermal analysis, an optimised thermal cycle was set up, which involved the debonding step at 560 °C for 1 h in flowing air, to allow a good decomposition of the organic matrix, and the sintering step at 900 °C for 1 h in flowing carbon dioxide, to avoid an excessive loss of the carbonate from the apatitic structure.

The density of the porous bodies was measured by geometric weight/volume evaluation (so-called apparent density). The open microporosity distribution was evaluated by Hg porosimeter (Porosimeter 2000, Carlo Erba, Milan, Italy).

The compressive strength of the sintered CHA porous bodies was measured on cylindrical specimens 10 mm×7 mm (height×diameter) using an Instron machine model 1195 (High Wycombe, Bucks, UK) with a crosshead speed of 0.5 mm/min. To avoid shear stress concentration, a thin foil was inserted between each end of the cylinder and the loading plates of the machine. The compressive strength was calculated from the maximum load registered during the test divided by the original area (six specimens were tested).

In vivo tests were carried out on six New Zealand White type rabbits. A blind tunnel (4 mm of diameter) in the metaepiphyseal distal zone of the femur was created aseptically. This tunnel was then filled with a

properly shaped cylinder of porous CHA using the "in press-fit" technique, to assure loads similar, as much as possible, to physiological ones. Similarly, a porous cylinder of HA was inserted in the left femur of the animals, as a control. The animals were not immobilised during the postoperative period and two of them were sacrificed 1 month after the surgery.

The proximal third of the right tibia of each rabbit was removed and fixed in 10% buffered formaldehyde for 5 days, then embedded in paraffin for 21 days, and then cut to a thickness of 6 μm. Toluidine blue was used as staining. The specimens were subjected to X-rays, light microscope and histomorphometric evaluation.

3. Results and discussion

The yield of the synthesis process was about 15 g of CHA powder per synthesis. The ICP-OES analysis yielded a Ca/P molar ratio of 2.01 ± 0.02, which is higher than the stoichiometric value (1.667), indicating the presence of B-type carbonate substituted hydroxyapatite. In particular, considering the B-CHA chemical formula $Ca_{10-x/2}(PO_4)_{6-x}(CO_3)_x(OH)_2$ and the Ca/P value, a x value of 1.36 was calculated, corresponding to about 8.8 wt% of B-carbonate per mol of B-CHA ($Ca_{9.32}(PO_4)_{4.64}(CO_3)_{1.36}(OH)_2$, molecular weight 929.94 g/mol).

The XRD analysis of the as prepared CHA powder, revealed no secondary phases (Fig. 1) besides the apatitic phase, but detected a variation of the unit cell parameters of the powder compared to stoichiometric HA; a decrease in the a parameter from 9.4180 (ICDD card n.9-432) to 9.3780(5) Å and an increase in the c parameter from 6.8840 (ICDD card n.9-432) to 6.9025(5) Å. Thus the c/a ratio increased from 0.7309 (HA) to 0.7361(1), indicating the formation of a B-carbonated hydroxyapatite.

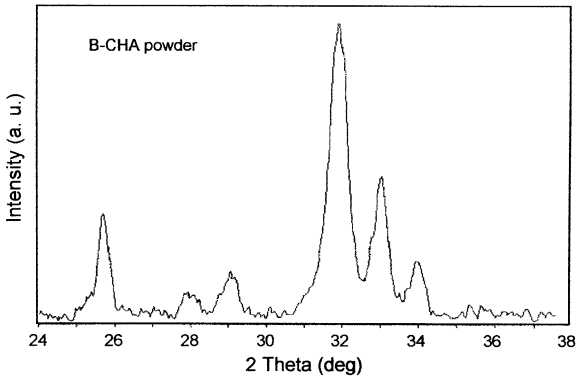

Fig. 1. XRD pattern of B-CHA powder, showing only the apatitic peaks (CuK_α radiation); the overlapping of the (211) and (112) peaks at 2 θ≈32 is typical of carbonated hydroxyapatite.

The degree of crystallinity of the powder was about $72 \pm 5\%$, evaluated by an XRD method elsewhere proposed.[10]

A quantitative XRD method using literature data[5] to establish an interpolation curve was used to correlate the cell parameter ratio c/a with the B-type carbonate content (as stoichiometric coefficient value x) (Fig. 2). This curve, was fitted to the following equation

$$x = 6(30.383\ \ c/a - 22.208)^{3/4}$$

which was then utilised to determine the B-carbonate content of the synthesised CHA powders from the XRD analysis results. Following this method, $x = 1.47(3)$ was calculated, corresponding to about 9.5 wt.% of carbonate substituting the phosphate site. Considering the experimental errors, these values are in satisfactory agreement with those found starting from ICP data ($x = 1.36(3)$, 8.8 wt.% B-carbonate).

The FTIR analysis (Fig. 3) detected strong peaks at the wavenumbers of the B-type CHA (870, 1430 and 1450 cm^{-1}). The typical peaks of the A-type CHA (880, 1450 and 1540 cm^{-1}) were not evident, but the presence of carbonate substituting in the hydroxyl site was highlighted by the deconvolution analysis of the 880 and 870 cm^{-1} peaks; from the peak area ratio, the A/B ratio was evaluated as about 0.1. Starting from the C amount detected by the elemental analyser, the total A + B carbonate was evaluated as 10.5 wt%. Therefore the contribution of the A-type carbonate (⩽1 wt.%) can be neglected.

The TG analysis of the CHA powder was performed up to 1450 °C in flowing CO_2, using a heating rate of 10 °C/min (Fig. 4). The weight loss up to about 300 °C is due to removal of adsorbed water or carbon dioxide. The second weight loss of about 8.5 wt.% (from 700 to

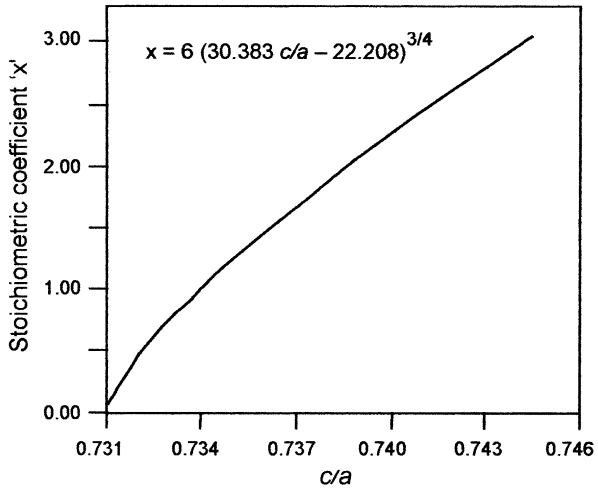

Fig. 2. Stoichiometric coefficient 'x' of B-type carbonate in the B-CHA chemical formula $Ca_{10-x/2}(PO_4)_{6-x}(CO_3)_x(OH)_2$ versus unit cell parameters c/a ratio (behavior drawn on the basis of literature data).[5]

1450 °C) is due to the carbonate decomposition and to the dehydroxylation of the CHA powder. Considering that both the phenomena occur gradually over a wide range of temperatures,[11–13] it is impossible to assign them to specific loss steps of the TG curve. But, taking into account that the contribution of the dehydroxylation is about 1.9 wt.%, the carbon dioxide loss due to decarbonation should be about 6.6 wt.%, that corresponds to a carbonate amount of about 9 wt.% in the starting CHA powder. Such a value is in good agreement with those calculated starting from both the XRD and ICP data.

The granulometric evaluation was performed on the as-prepared CHA powder by X-ray sedimentography and the mean particle size was ≈0.55 μm with the most frequent size at 0.25 μm. Such a value referred to the agglomerate dimension, following the ultrasound treatment performed before the analysis, in order to disaggregate the powder. The SEM images showing the morphology of the as prepared CHA powder (Fig. 5 a,b), showed that the primary particles were submicrometer in size (about 70–100 nm), with a high tendency to agglomerate. The specific surface area determined by the B.E.T method was 51 ± 3 m^2/g, which value is consistent with an average particle size of about 20 nm, i.e about 25 times lower than 0.55 μm (the mean particle size detected by sedimentography), but in agreement with the submicrometer size detected by SEM. The B.E.T value is higher than that (about 30 m^2/g) for the high crystallinity HA powder produced at 90 °C via neutralisation route.[8] The higher B.E.T value can be due to lower size of the primary particles as well as to a closed porosity inside them.

The electrokinetic behaviour of the suspension of the CHA powder vs pH was studied in comparison with two HA powders (Fig. 6), characterised by different values of the crystallinity degree (Xc) and specific surface area (s.s.a). HALA: s.s.a ≈ 120 m^2/g and Xc≈20%; HAHA: s.s.a≈35 m^2/g and Xc≈80%.[8,14]

Even if the s.s.a (≈51 m^2/g) and Xc (≈70%) values of the CHA are more similar to those of HAHA powders, the behaviour of the suspension of CHA is more similar to that of HALA. In particular the stability range for CHA and HALA is shifted towards higher pH values than HAHA. Natural pH and isoelectric point are higher for CHA and HALA with respect to HAHA.

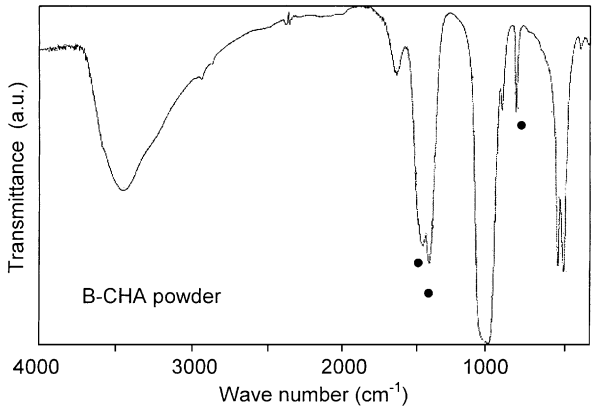

Fig. 3. FTIR pattern of B-CHA powder, showing the characteristic peaks of carbonate group (•) besides those of HA.

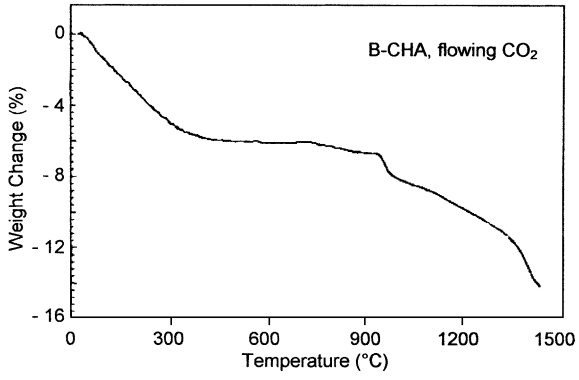

Fig. 4. Weight change vs temperature for TG analysis of the B-CHA powder performed at 10 °C/min up to 1400 °C in flowing CO_2.

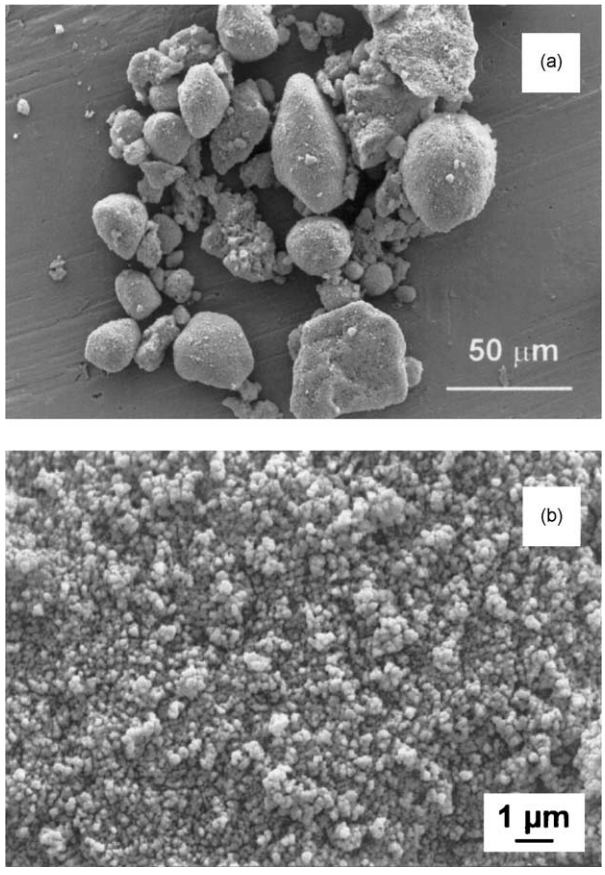

Fig. 5. SEM micrographs showing the morphology of the B-CHA powder: the powder tends to form agglomerates (a), which are constituted by nanosized primary particles (b).

Probably, the presence of carbonate group changes the surface behaviour of the powder, giving rise to a higher basic hydrolysis: the compositional difference compensates for the difference in the surface reactivity due to the s.s.a values, making the behaviour of CHA very close to that of HALA.

Sintering tests were performed to identify the best sintering conditions, in order to allow a sufficient carbonate residue, limit the formation of secondary phases and also to assure a good densification.

The XRD analysis showed that the carbonate residue was about 3 wt.% ($c/a = 0.7320(1)$, i.e. $x \approx 0.5$) in the CHA powder after calcining at 1030 °C for 2 h and that 4.5 vol.% of CaO also formed. Decreasing the sintering temperature to 950 and 900 °C, the carbonate amount retained in the apatitic structure was about 5.3 and 6.3 wt%, respectively ($c/a = 0.7335(1)$ and $0.7340(1)$, i.e. $x \approx 0.85(2)$ and $1.00(2)$, respectively); the CaO amount resulted about 4 and 2.5 vol.%, respectively.

The optimized thermal treatment of the dried porous bodies included a debonding step at 560 °C for 1 h under flowing air, in order to favour the cellulosic matrix decomposition and the sintering step at 900 °C for 1 h under flowing carbon dioxide, in order to prevent the carbonate loss from the material as well as avoid CaO formation but assuring the densification of the samples. The sintering temperature was about 350 °C lower than that (1250 °C) of analogous HA samples,[8,9] confirming the ability of the substituting carbonate to decrease the densification temperature of the hydroxyapatite.[10]

After sintering the ceramic resembled the cellulose matrix texture, giving rise to a structure characterised by several macropores, whose size (> 100–200 μm) can assure osteoconduction after implantation (Fig. 7 a,b). At high magnification the walls of the meso and macropores

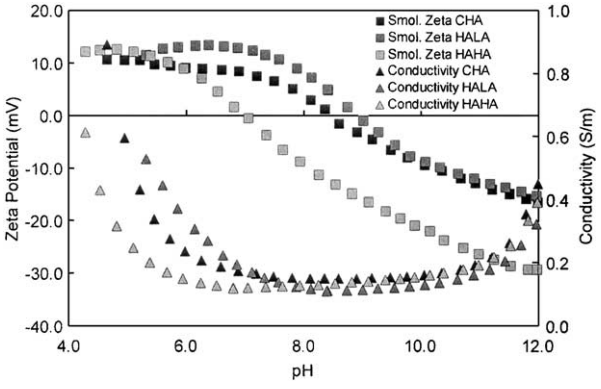

Fig. 6. Zeta potential and conductivity vs pH for the B-CHA powder suspension compared to HA with different values of the crystallinity degree (Xc) and specific surface area (s.s.a). (B-CHA: s.s.a≈51 m^2/g and Xc≈70%, HALA: s.s.a≈120 m^2/g and Xc≈20%; HAHA: s.s.a≈35 m^2/g and Xc≈80%). Even if the values of the CHA are more similar to those of HAHA powder, the behavior of the suspension of CHA is more similar to that of HALA.

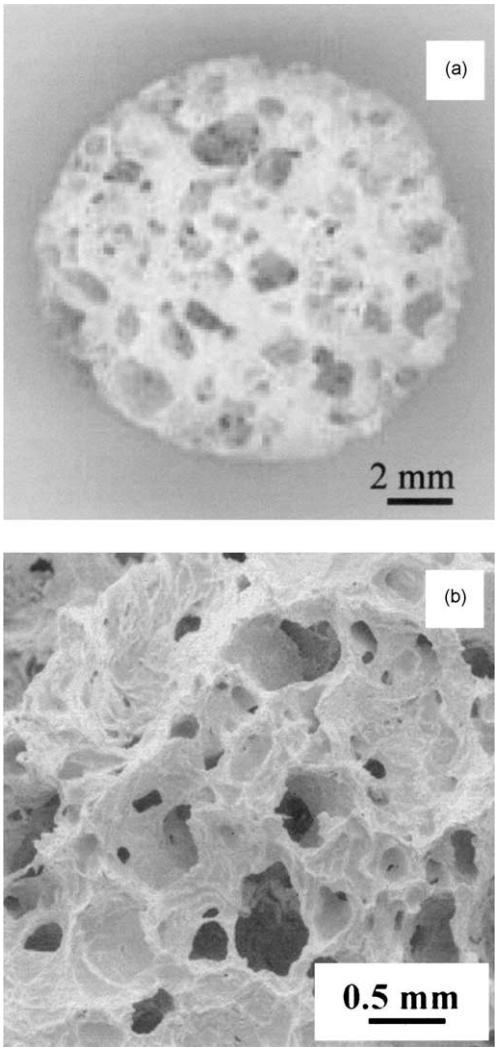

Fig. 7. SEM micrographs showing the morphology of the sintered B-CHA porous sample: low magnification image of the equatorial section (a) and high magnification image showing interconnected pores of different size (b). The macropores (> 100–200 μm) can assure the osteoconduction process, while the meso- and micropores (not visible at this magnification) can assure the physiological fluid distribution inside the ceramic after implantation.

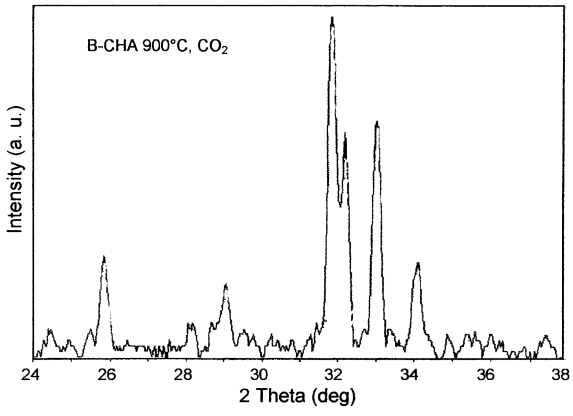

Fig. 8. XRD pattern from the sintered B-CHA porous samples, showing only the carbonate- apatitic peaks (CuK_α radiation).

showed a diffuse microporosity (< 10 μm in size), which help to increase the interconnetion degree and allow the physiological fluids to enter the inner part of the sample. The open microporosity was estimated by Hg porosimetry as about 9%. The total porosity of the porous body was evaluated from the density value calculated as weight/volume and amounted to 45%.

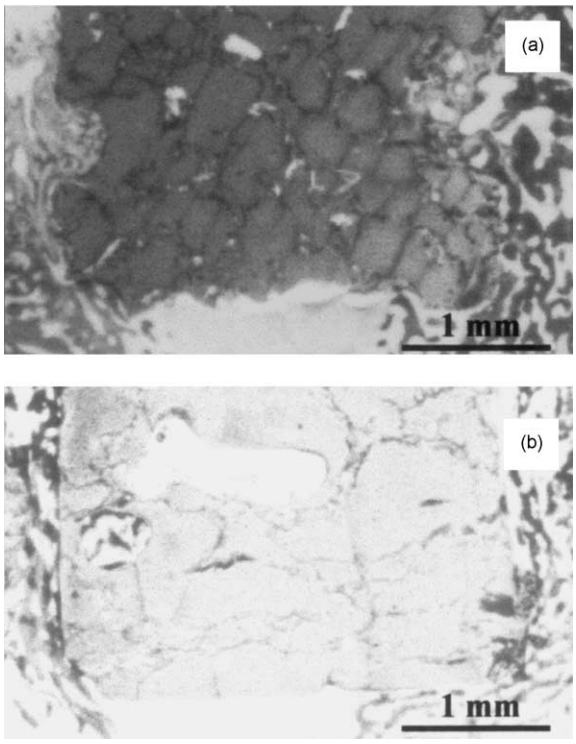

Fig. 9. In vivo test results after 1 month: optical micrographs (low magnification) of the porous B-CHA implant (a) showing a discontinuous/disgregated morphology, compared to HA (b).

The XRD analysis of the sintered bodies (Fig. 8) confirmed the absence of secondary phases and estimated the residual carbonate amount in the apatitic structure as about 6 wt% (from c/a value, x≈1, as reported above).

The compressive strength of the porous samples resulted 6.0±0.5 MPa, which is a higher value than that (3.1±0.3 MPa) found for analogous samples prepared with HA. The CHA was characterised by higher efficiency of densification, which makes the struts between the pores less brittle compared to those of the HA porous samples. In fact, the morphology of the struts strongly influenced the mechanical properties together with the microporosity, surely more than the macroporosity did.[8]

In vivo tests showed that, after one month from implantation, both the CHA and HA porous implants caused no infections and strong adhesion between bone and the bioceramics was observed. Good osteointegration between the cortical and the spongy bone and the bioceramics also was detected. Moreover, compared to HA, the porous CHA implant showed a higher X-ray transparency, probably due to intrinsic characteristics of the material.

In the rabbit model, the discontinuous morphology of the CHA implant after 1 month, indicated an initial fragmentation/disgregation of the ceramic, imputable to earlier bioresorption, with respect to HA (Fig. 9 a,b low magnification). Moreover, a higher presence of newly formed bone and higher osteogenesis inside macropores was also observed in the CHA case compared to HA (Fig. 10 a,b).

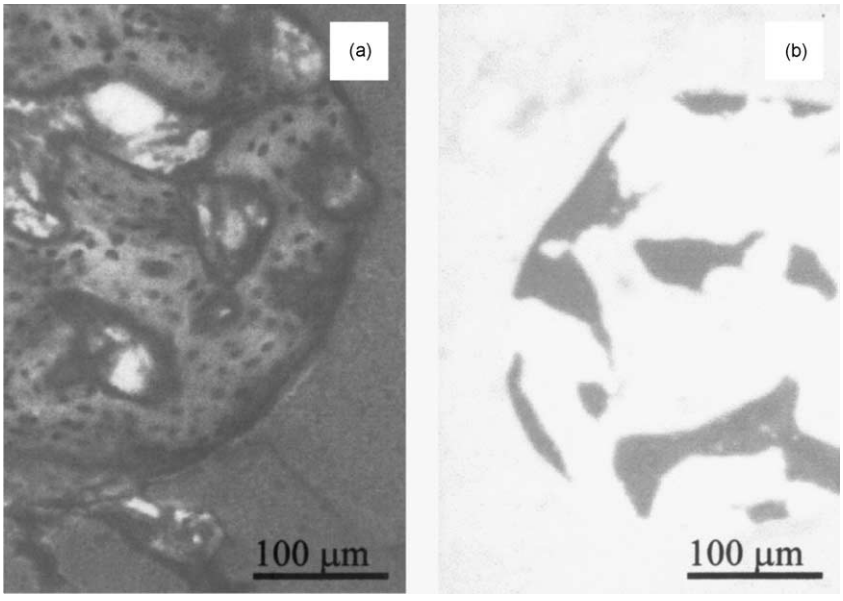

Fig. 10. In vivo test results after 1 month: optical micrographs (high magnification) showing a higher presence of newly formed bone and a higher osteogenesis inside a macropore (≈300 μm in size) in the case of the porous B-CHA implant (a) compared to HA one (b).

The presence of an intimate adhesion between the newly osteogenetic tissue and the CHA bioceramic and the presence of osteoclastic cells meant an intensive activation of the BMU (Bone Morphogenetic Units), which seem to attack and erode somewhere the CHA surface.

In the case of CHA, the newly formed bone was characterized by thicker bone trabeculae, and showed the initial formation of the Haversian channels and lamellar structures, typical of mature bone.

4. Conclusions

Highly pure powder of B-type carbonated hydroxyapatite powder with nanosize dimensions, was produced via wet-chemical synthesis. Comparing the results arising from different analysis techniques, the carbonate content was estimated to be about 9 wt%.

A forming process, based on an impregnation technique, was optimised in order to produce porous structures with proper pore size and distribution, which mimic the morphology of the spongy bone and allows bone ingrowth.

The sintering cycle was optimised (900 °C, CO_2 atmosphere) for the production of porous bodies of synthetic B-type CHA, characterised by a carbonate amount very close to that of the biological carbonated hydroxyapatite.

The compressive strength of the CHA porous bodies was about twice the strength of analogous porous samples of HA. The mechanical resistance is therefore less critical for porous CHA structures, even if sintered at temperature about 350 °C lower than HA.

The first results of in vivo tests on NZW rabbits showed good biocompatibility and osteointegration of the CHA implants, with higher osteoconductive properties and earlier bioresorption, compared to similar HA samples, used as control. In the CHA samples, the quantity of newly formed bone was greater and showed earlier maturation as indicated by the Haversian channels and the lamellar structures.

References

1. Driessens, F. C. M., *Bioceramics of Calcium Phosphates*. CRC Press, Boca Raton, FL, 1983.
2. Rey, C., Renugopalakrishnan, V., Collins, B. and Glimcher, M., Fourier transform infrared spectroscopic study of the carbonate ions in bone mineral during aging. *Calcif. Tissue Int.*, 1991, **49**, 251–258.
3. Burnell, J. M., Teubner, E. J. and Miller, A. G., Normal maturational changes in bone matrix, mineral, and crystal size in the rat. *Calcif. Tissue Int.*, 1980, **31**, 13–19.
4. Rey, C., Collins, B., Goehl, T., Dickson, I. R. and Glimcher, M., The carbonate environment in bone mineral: a resolution-enhanced Fourier transform infrared spectroscopy study. *Calcif. Tissue Int.*, 1989, **45**, 157–164.
5. Le Geros, R. Z., Calcium phosphates in oral biology and medicine. In *Monographs in Oral Science*, ed. H. Myers Karger. AG Publishers, Basel, 1991, pp. 82–107.
6. Redey, S. A., Razzouk, S., Rey, C., Bernache-Assollant, D., Leroy, G., Nardin, M. and Cournot, G., Osteoclast adhesion and activity on synthetic hydroxyapatite, carbonated hydroxyapatite and natural calcium carbonate: relationship to surface energies. *J. Biomed. Mater. Res.*, 1999, **45**, 140–147.
7. Redey, S. A., Nardin, M., Bernache-Assolant, D., Rey, C., Delannoy, P., Sedel, L. and Marie, P. J., Behavior of human osteoblastic cells on stoichiometric hydroxyapatite and type A carbonate apatite: role of surface energy. *J. Biomed. Mater. Res.*, 2000, **50**, 353–364.
8. Guicciardi, S., Galassi, C., Landi, E. and Tampieri, A., Rheological characteristics of slurry controlling the microstructure and the compressive strength behavior of biomimetic hydroxyapatite. *J. Mater. Res.*, 2001, **16**, 163–170.
9. Tampieri, A., Celotti, G., Sprio, S., Delcogliano, A. and Franzese, S., Porosity-graded hydroxyapatite ceramics to replace natural bone. *Biomaterials*, 2001, **22**, 1365–1370.
10. Landi, E., Tampieri, A., Celotti, G. and Sprio, S., Densification behaviour and mechanisms of synthetic hydroxyapatites. *J. Eur. Ceram. Soc.*, 2000, **20**, 2377–2387.
11. Rey, C., Calcium phosphates for medical applications. In *Calcium Phosphates in Biological and Industrial Systems*, ed. Z. Amjad. Kluwer Academic Publishers, Boston, MA, 1998, pp. 217–239.
12. Zyman, Z., Cao, Y. and Zhang, X., Periodic crystallization effect in the surface layers of coatings during plasma spraying of hydroxyapatite. *Biomaterials*, 1993, **14**, 1140–1144.
13. Wang, C. K., Ju, C. P. and Chern Lin, J. H., Effect of doped bioactive glass on structure and properties of sintered hydroxyapatite. *Mat. Chem. Phys*, 1998, **53**, 138–149.
14. Pretto, M., Costa, A. L., Landi, E., Tampieri, A. and Galassi, C., Dispersing behavior of hydroxyapatite powders produced by wet chemical synthesis. *J. Am. Ceram. Soc.*, in press.